RSC Advances

PAPER

View Article Online
View Journal | View Issue

Cite this: *RSC Adv.*, 2015, **5**, 66067

Non-corrosive green lubricants: strengthened lignin–[choline][amino acid] ionic liquids interaction *via* reciprocal hydrogen bonding

Liwen Mu,[a] Yijun Shi,*[b] Xiaojing Guo,[c] Tuo Ji,[a] Long Chen,[a] Ruixia Yuan,[ad] Logan Brisbin,[a] Huaiyuan Wang[d] and Jiahua Zhu*[a]

Received 11th June 2015
Accepted 15th July 2015

DOI: 10.1039/c5ra11093a

www.rsc.org/advances

A series of novel green lubricants with dissolved lignin in [choline][amino acid] ([CH][AA]) ionic liquids (ILs) have been synthesized in this work. The effect of lignin on the thermal and tribological properties of the lignin/[CH][AA] lubricants was systematically investigated by means of thermogravimetric analysis, differential scanning calorimetry, and a friction and wear tester. The lignin in [CH][AA] has been demonstrated to be an effective additive to improve thermal stability, reduce the wear rates and stabilize the friction coefficients of lignin/[CH][AA] lubricants. Density function theory calculations on the electronic structure of [CH][AA] ILs reveal the atomic natural charge of ILs and their hydrogen bonding capability with lignin. Moreover, these green lubricants show excellent anti-corrosive properties against commercial aluminum and iron boards. The strong physical adsorption of [CH][AA] ILs onto the steel surface and the reciprocal hydrogen bonding between [CH][AA] ILs and lignin synergistically contribute to the enhanced lubrication film strength and thus the tribological properties of these new lubricants. This work provides a new perspective on utilizing complete bio-products in advanced tribological lubrication systems. In addition, this will open a new application venue for lignin to improve product value in lignocellulosic biomass utilization.

Introduction

Ionic liquids (ILs) have been defined as molten salts that are entirely ionic in nature, comprising both cationic and anionic species with a melting point below 100 °C.[1] ILs are widely used as electrolytes in electrochemistry, solvents, extractants and catalysts in organic synthesis due to their large charge density, excellent electrochemical stability, low/negligible volatility, tunable polarity *etc.*[2,3] However, the major disadvantages of conventional ILs, such as high cost, potential toxicity, poor biodegradability and corrosivity[4–7] especially those with imidazolium or pyridinium cations and halogen anions, have been well recognized in recent years which restrict their wider applications considering the economic feasibility and environmental sustainability. ILs synthesized from renewable bio-resources, also named 'Green ILs', are attracting increasing interest from researchers with significant advantages of biodegradability, non-toxicity, environmentally benign features and more importantly their comparable physicochemical properties with conventional ILs.[4,8]

Choline, an essential nutrient for the synthesis of constructional components in cell membranes, is known to widely exist in nature and is certainly biodegradable.[9] Amino acids, composed of amine and carboxylic acid functional groups along with a side-chain specific to each amino acid, are also one of the most abundant organic compounds in nature.[10] Both choline and amino acids are important feed-stocks for the synthesis of green ILs.[11,12] Recently, different types of [choline][amino acid] ([CH][AA]) have been synthesized[13] and used in biomass pretreatment processes.[14] Other similar 'Green ILs' have found applications in the fields of lubrication,[15] catalysis,[16] carbon dioxide capture[17] *etc.*

Use of ILs as high performance synthetic lubricants started from 2001.[18] The major advantages of ILs over petroleum oil based lubricants are their distinct physicochemical characteristics, such as negligible vapour pressure, high polarity and non-flammability.[19] Over the past years, the major efforts of exploring IL lubricants in tribological systems are devoted to halogen-containing ILs (such as $[BF_4]^-$, $[PF_6]^-$),[20,21] which are easily hydrolysed by moisture from processing fluids and generate highly toxic and corrosive hydrogen fluoride.[22] Besides, ILs meet significant challenges when operated in severe conditions such as oxidative, high temperature environments

[a]*Intelligent Composites Laboratory, Department of Chemical and Biomolecular Engineering, The University of Akron, Akron, OH 44325, USA. E-mail: jzhu1@uakron.edu; Tel: +1-330-972-6859*

[b]*Division of Machine Elements, Luleå University of Technology, Luleå, 97187, Sweden. E-mail: yijun.shi@ltu.se; Tel: +46-920492064*

[c]*Shanghai Institute of Applied Physics, Chinese Academy of Sciences, Shanghai 201800, P. R. China*

[d]*College of Chemistry and Chemical Engineering, Northeast Petroleum University, Daqing 163318, P. R. China*

and high frequency oscillating movement under high pressure.[7,23]

Lignin, a cross-linked polymer with phenylpropane monomers, is the second most abundant biopolymer in nature. In the pulp and paper industry, lignin is usually considered as a by-product or even waste, which is directly burnt as a low grade fuel to recover energy.[24] However, taking advantage of the unique molecular structure, lignin can be processed into valuable functional additives in composite materials with appropriate surface modification.[25] For example, the rigid molecular structure and abundant surface functional groups of lignin well qualifies it as a reinforce filler/cross-linker to improve mechanical properties of various polymers including but not limited to epoxy,[26] silicone elastomers,[27] and poly(lactide).[28] In addition, lignin has been demonstrated as an excellent antioxidant arising from its phenolic structures.[29,30] However, to the best of our knowledge, the usage of lignin as a lubricant additive has rarely been studied especially in 'Green ILs'.

In this work, we synthesized two 'Green ILs', [choline][glycine] and [choline][L-proline] with choline as the cation and two amino acids, glycine and L-proline, as the anion respectively, and used them as the base to develop high performance lignin promoted green lubricants. Taking advantage of the thermally stable features and anti-oxidative properties of lignin (one of the most important performance indicators for lubricants) as well as its strong bonding with [CH][AA] ILs through reciprocal hydrogen bonding, it is anticipated that the tribological properties of lignin/[CH][AA] green lubricants will be significantly improved. The anti-corrosive properties of pure [CH][AA] ILs and lignin/[CH][AA] are also investigated in this work.

Experimental

Materials

Choline hydroxide aqueous solution (48–50 wt% in water) was purchased from Tokyo Chemical Industry. Glycine (≥99%), L-proline (≥99%), and deuteroxide (D_2O, 99.9 atom% D), alkali lignin were purchased from Sigma Aldrich. 1-Butyl-3-methylimidazolium chloride ([BMIm]Cl, >99%; water content, <1000 ppm) was purchased from center for green chemistry and catalysis of Lanzhou Institute of Chemical Physics, Chinese Academy of Sciences. [BMIm]Cl was dried overnight *in vacuo* at 70 °C before use. All chemicals were used as received without further treatment.

Synthesis of ILs and lignin/ILs

Choline hydroxide aqueous solution was added dropwise to equimolar glycine or proline amino acid with ice cooling. Then, the mixture was magnetically stirred at room temperature for 48 h. After reaction, the water in the mixture was removed using a rotary evaporator at 60 °C. Finally, the [choline][glycine] (IL1) and [choline][L-proline] (IL2) were dried *in vacuo* for 48 h at 70 °C, refer to Scheme 1 for their molecular structures. Alkali lignin of different weight fractions (1, 3, 5 and 7 wt%) was added to IL1 at 90 °C and stirred for 24 h with N_2 protection, which eventually formed homogeneous solutions which are denoted as IL1-1, IL1-3, IL1-5 and IL1-7. Same procedure was applied to IL2 to prepare the IL2-1, IL2-3, IL2-5 and IL2-7 lubricants.

Characterization

The molecular structures of IL1 and IL2 were analysed by proton nuclear magnetic resonance (^{1}H NMR, Varian Mercury-300) in D_2O at 300 MHz. The following abbreviations are used to designate multiplicities: s = singlet, d = doublet, t = triplet and m = multiplet. IL1: d = 3.99–4.08 (d, 2H, CH_2), 3.45–3.54 (m, 2H, CH_2), 3.22–3.32 (m, 2H, CH_2–N), 3.18 ppm (s, 9H, CH_3, CH_3, CH_3). IL2: d = 3.98–4.07 (m, 2H, CH_2), 3.39–3.56 (m, 3H, CH–N, CH_2), 3.16 (s, 9H, CH_3, CH_3, CH_3), 3.01–3.10 (m, 1H, CH_2–N), 2.68–2.84 (m, 1H, CH_2–N), 2.02–2.10 (t, 1H, CH_2), 1.62–1.78 (d, 3H, CH_2, CH_2). All these characterization results are well consistent with the previous literature report,[4] which indicates the successful synthesis of the desired ILs. The thermal decomposition temperatures (T_d) of the ILs and lignin/IL (1, 3, 5 and 7 wt% lignin in the ILs) were determined by thermogravimetric analysis (TGA, TA instrument Q500) in N_2 and air atmosphere from 20 to 500 °C with a heating rate of 10 °C min^{-1}. The glass transition temperature (T_g) was determined with a differential thermal analyzer (DSC, TA Instruments Q2000) from −150 °C to 100 °C with a heating rate of 10 °C min^{-1} after cooling samples to −150 °C in an aluminum pan. An Optimol SRV-III oscillating friction and wear tester was used to evaluate tribological properties of the green lubricants under boundary lubrication conditions based on the ASTM D 6425 protocol. During the test, the upper steel ball (52100 bearing steel, diameter 10 mm, surface roughness (R_a) 20 nm) slides under reciprocating motion against a stationary steel disc (100CR6 ESU hardened, Ø24 mm × 7.9 mm, and surface roughness (R_a) 120 nm). The disc was supplied by Optimol Instruments Prüftechnik GmbH, Germany. The ball was provided by SKF, Sweden. Before each test the device and specimens were cleaned with acetone and ethanol. All tests were conducted under the load of 150 N (2.5 GPa maximum Hertzian pressure) and 258 N (3 GPa maximum Hertzian pressure) at room temperature (25 °C), a sliding frequency of 50 Hz, and an amplitude of 1 mm. The friction coefficient curves were recorded automatically with a data acquiring system linked to the SRV-III tester. After the tests the wear volumes of the lower discs were determined using an optical profiling system (Zygo 7300). The anti-corrosive properties of IL and lignin/ILs were studied on aluminum and iron metal boards by visual comparison before and after the corrosion experiments. The test was performed at 100 °C for 6 h in an oven with a drop of testing liquid

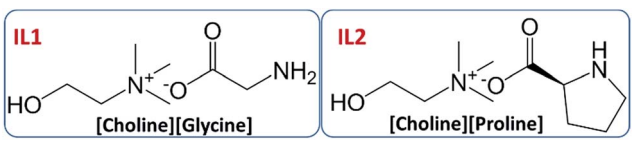

Scheme 1 Molecular structures of [choline][glycine] and [choline][L-proline].

on the metal board. Upon completing the test, the metal boards were cooled down to room temperature and washed with DI water for corrosion spot detection. The optical images of the corrosion spot were recorded by a microscope (Novel optics Instruments NJF-120A).

DFT calculations

Electronic structure calculations on both IL1 and IL2 were performed with the Gaussian 09 C1 package[31] using density functional theory (DFT) at the B3LYP level of theory.[32,33] 6-31++G* basis sets were used for carbon, nitrogen, oxygen, and hydrogen atoms. Frequency calculations were performed to verify that the geometries were minimal.

Results and discussion

Fig. 1 shows the thermal degradation and derivative thermogravimetry (DTG) curves of [CH][AA] ILs with different fractions of lignin in N_2 atmosphere. The onset decomposition temperature (T_{onset}) of the lignin/[CH][AA] in both N_2 and air are summarized in Table 1. The T_{onset} of IL1 is obviously lower than IL2, which is attributed to the thermally stable pyrrolidine structure in the anion of IL2.[4] Besides, lignin is effective in improving the T_{onset} of both IL1 and IL2 under N_2 and air atmospheres due to the thermally stable phenolic groups in lignin.[34]

DSC results in Fig. 2 and Table 1 reveal that these lignin/[CH][AA] ILs do not show melting behavior in the measured temperature range, but exhibit typical glass transition phenomena (T_g) ranging from −47.8 to −13.7 °C. For IL1, the T_g increases from −47.8 to −13.7 °C with the addition of lignin, indicating the stronger cation–anion attraction force after adding lignin. The lignin provides protons from its hydroxyl groups that form hydrogen bonds with the amine groups from the anions of IL1. Besides, the proton from the hydroxyl group of the cation has the capability to form a hydrogen bond as well with ether groups in lignin. Through this reciprocal interaction between IL1 and lignin, the molecular interactions of cation–anion, cation–lignin and anion–lignin could be enhanced and therefore larger T_g was observed in lignin/IL1. Similar strengthened cation–anion attractions by substituting smaller volume, lower molecular weight and symmetric cation or anion and thus enhanced T_g have been reported in other ILs.[35] It is worth mentioning that IL1-7 shows lower T_g = −27.4 °C than that of IL1-5 probably due to the weakened interactions between IL and lignin with the existence of an excess amount of lignin. Unexpectedly, the addition of lignin in IL2 decreases the T_g of lignin/IL2 by 5–9 °C probably due to the weaker lignin–IL2 interaction that has been proved by DFT calculations in a later section.

The wear and friction properties of the lignin/ILs were investigated using a steel ball on steel disc configuration since steel is the most widely used material in industry. Fig. 3 shows the friction coefficient evolution during 1 hour friction test with

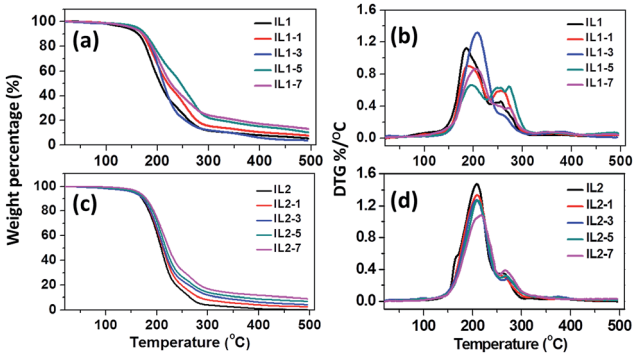

Fig. 1 (a) TGA, (b) DTG curves of lignin/[CH][AA] ILs under N_2 atmosphere. IL1-1, IL1-3, IL1-5 and IL1-7: 1, 3, 5, 7 wt% lignin/[choline][glycine]; IL2-1, IL2-3, IL2-5 and IL2-7: 1, 3, 5 and 7 wt% lignin/[choline][proline].

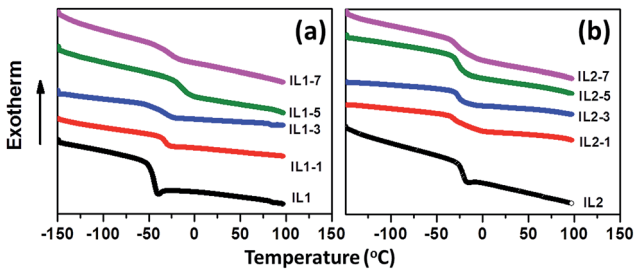

Fig. 2 DSC curves of lignin/[CH][AA] ILs.

Table 1 Thermal properties of lignin/[CH][AA] ILs

Samples	T_{onset,N_2} (°C)	$T_{onset,air}$ (°C)	T_g (°C)
IL1	163.9	165.8	−47.8
IL1-1	166.3	170.8	−33.1
IL1-3	180.1	166.9	−31.7
IL1-5	168.3	167.8	−13.7
IL1-7	171.5	171.0	−27.4
IL2	175.6	178.6	−23.2
IL2-1	175.6	182.1	−32.1
IL2-3	175.3	180.8	−27.1
IL2-5	176.8	175.4	−28.4
IL2-7	178.1	179.2	−29.3

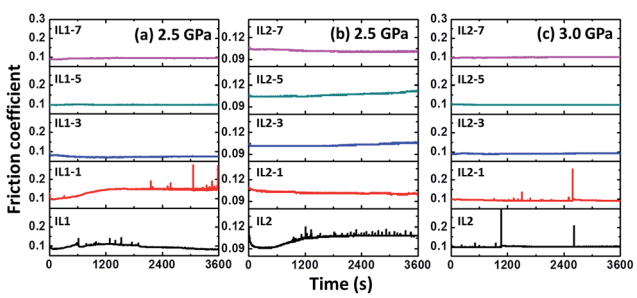

Fig. 3 Friction coefficient evolution by using different lubricants. (a) IL1 series at 2.5 GPa, (b) IL2 series at 2.5 GPa, and (c) IL2 series at 3.0 GPa.

the presence of lignin/[CH][AA] lubricants. It is well recognized that the testing pressure of 2.5 GPa is beyond the normal industrial operation pressure, not to mention the 3.0 GPa tested in this work. Apparently, unstable friction coefficients were observed when using pure IL1 and IL2 as lubricants, Fig. 3. The friction coefficient can be stabilized at or below 0.1 by adding 3–7 wt% lignin into both IL1 and IL2, Fig. 3(a–c).

Fig. 4 shows the wear volume losses of the discs with different ILs and lignin/IL lubricants. The wear volume losses of the steel discs lubricated by lignin/IL1 are apparently lower than the one lubricated by pure IL1. Specifically, the wear volume of the disc lubricated by IL1-7 is only 27% of the one lubricated by pure IL1. For IL2 based lubricants, it is quite clear that the addition of lignin also improves the anti-wear properties. Comparing the tribological results of the two pure ILs, the anti-wear performance of IL2 is relatively better than IL1, which is attributed to the larger adsorption capability of IL2 onto the metal surface.[36] To explore the potential of IL2 and lignin/IL2 in extreme pressure conditions, tribological tests were further conducted under the higher pressure conditions at 3.0 GPa. It is observed that the wear volume loss decreases continuously with increasing lignin fraction in the IL2. In terms of friction stabilization and anti-wear protection, [CH][AA] ILs with 3–7 wt% lignin fractions seem excellent lubricants for steel/steel contacts even at high pressure conditions.

Fig. 5 presents the three-dimensional (3D) morphology of the corresponding wear tracks on discs after friction testing. From Fig. 5(a–e), the wear track with IL1 is obviously deeper than the tracks with lignin/IL1. Comparing the 3D images from the first and second rows of Fig. 5, the IL1 based lubricants show relatively larger and deeper wear tracks than IL2 based lubricants, which further confirms the superior anti-wear properties of IL2 under 2.5 GPa. Fig. 5(k–o) present the 3D images of wear tracks under 3.0 GPa with IL2 based lubricants, which show obviously deeper and larger wear tracks comparing the images obtained at 2.5 GPa. All the above results indicate that: (1) IL2 serves as a better lubricant base than IL1 in the steel/steel contact friction configuration; (2) dissolved lignin in either IL1 or IL2 helps to stabilize the friction coefficient and alleviate wear loss of the contacting metal pairs; (3) higher lignin fraction in ILs seems beneficial to the overall performance of the tribological system.

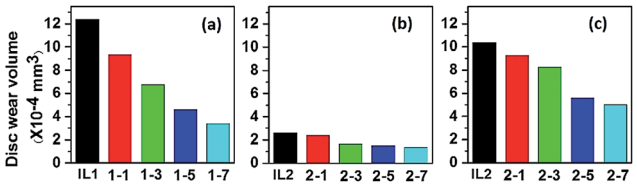

Fig. 4 Wear volume of disc lubricated by lignin/[CH][AA]. (a) IL1 series at 2.5 GPa, (b) IL2 series at 2.5 GPa, (c) IL2 series at 3.0 GPa. Testing duration: 1 h.

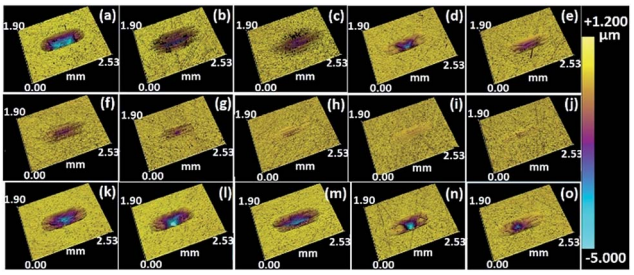

Fig. 5 The 3D microscopic images of wear tracks: (a–e) IL1, IL1-1, IL1-3, IL1-5 and IL1-7 at 2.5 GPa, (f–j) IL2, IL2-1, IL2-3, IL2-5 and IL2-7 at 2.5 GPa, (k–o) IL2, IL2-1, IL2-3, IL2-5 and IL2-7 at 3.0 GPa.

At the molecular scale, the excellent tribological properties of lignin/[CH][AA] green lubricants can be ascribed to two major contributions. Firstly, previous tribological study on amino acids based IL lubricants did not detect nitrogen element on the wear surfaces by XPS technique,[15] which excludes the occurrence of tribochemical reaction between the ionic liquid and metal surfaces. This also means the outstanding tribological properties of the [CH][AA] ILs are most likely attributed to the formation of IL films by physical adsorption during the friction process. During friction, low-energy electrons on the metal surface are released from contact convex sites, so the negatively charged carboxylic acid group in the amino acid exhibits strong affinity to the positively charged steel surface.[15] IL2 has demonstrated even stronger affinity to metal surfaces than IL1 in a previous literature report,[36] which positively contributes to the formation of a mechanically strong liquid film and thus effectively prevents direct contact between the steel ball and steel disc to reduce the friction coefficient and wear loss. Secondly, looking at the complex molecular structure of lignin, it is not difficult to see that proton donating groups (–OH) and proton accepting groups (–O–) widely exist in the lignin molecule. The nitrogen atom in the anion and the hydroxyl group in the cation tend to accept a proton from lignin (–OH groups) and donate a proton to lignin (–O– groups), respectively, thus reciprocal hydrogen bonds between lignin and [CH][AA] will be formed, Fig. 6. These reciprocal hydrogen bonds help to improve the mechanical strength of the lubrication film and result in effective interfacial separation between metal/metal contacts to reduce friction and wear.[15]

To have a better understanding of the hydrogen bonding between lignin and ILs, the electronic structures of the ILs were optimized using DFT calculations and the atomic charges were investigated by natural bond orbital (NBO) analysis at the B3LYP/B3LYP/6-31++G* level of theory, Fig. 7. On the basis of the natural population analysis (NPA), the natural charge of the nitrogen atom in the anion of IL1 is $-0.920\ e^-$, which is more negative than that of IL2 ($-0.717\ e^-$). That is to say, the hydrogen bond formation capability between IL1 and lignin is stronger than the one between IL2 and lignin. This also explains

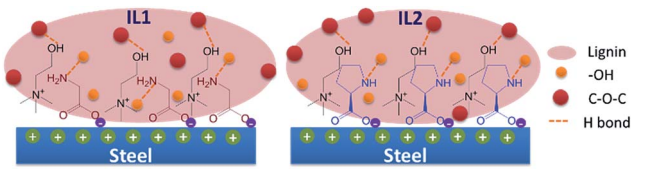

Fig. 6 Schematic illustration of physical adsorption of ILs onto a steel surface and reciprocal hydrogen bonding between lignin and ILs.

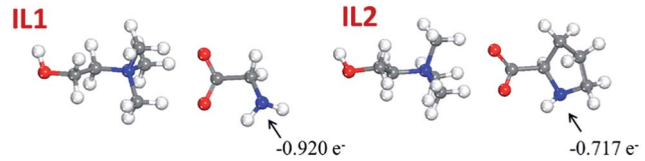

Fig. 7 Optimized structures and natural charges on the nitrogen atoms for IL1 and IL2 by the B3LYP method. (Red, white and blue balls represent oxygen, hydrogen and nitrogen atoms, respectively.)

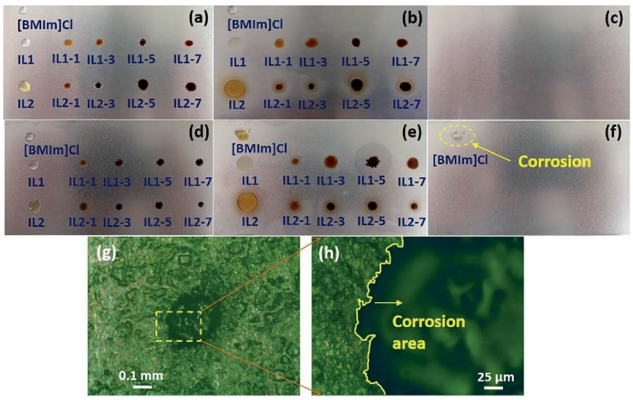

Fig. 8 Corrosion test photographs. Aluminum board: (a) liquid drops on plate, (b) after corrosion test, (c) after cleaning. Iron board: (d) liquid drops on plate, (e) after corrosion test, (f) after cleaning, dashed circle indicates the corrosion induced by [BMIm]Cl, (g) optical microscopic image of corrosion spot and (h) enlarged area at corrosion boundary.

the enhanced glass transition temperature and significantly reduced wear volume loss after incorporating lignin in IL1.

Lignin/IL lubricants in this work are expected to exhibit lower corrosivity than conventional ILs due to their completely bio-nature. Corrosion tests at 100 °C with 6 h duration were conducted to confirm this assumption. The conventional [BMIm]Cl IL is also tested for comparison. Fig. 8 shows the photographs of aluminum and iron boards before and after corrosion tests. The aluminum board retains the original surface features without corrosion from all the tested lignin/[CH][AA] and [BMIm]Cl, Fig. 8(a–c). Obvious corrosion occurred on the iron board by [BMIm]Cl, as seen in the dashed circled area in Fig. 8(f), while the rest of the iron board keeps its original surface features indicating the non-corrosive nature of all the lignin/[CH][AA] lubricants. Focusing on the corrosion spot formed by [BMIm]Cl, obvious pitting corrosion can be observed under an optical microscope, Fig. 8(g). The enlarged magnification at the edge area of the corrosion spot clearly distinguishes the boundary of uncorroded (left) and corroded (right) areas, Fig. 8(h). Overall, these new green lignin/IL lubricants exhibit outstanding anti-corrosive properties towards the most used metal materials.

Conclusion

To sum up, a series of novel green lubricants have been developed in this work using [CH][AA] ionic liquids as the lubricant base and strengthened by lignin through reciprocal hydrogen bonding in between. This work also presents a new application of lignin as an effective lubricant additive. The addition of lignin in [CH][AA] not only enhances the thermal stability, but also improves anti-wear properties and friction stability. The overall tribological performance is determined by the affinity of the ionic liquid to the metal surface and the strength of the ionic liquids–lignin interactions by hydrogen bonding. DFT calculations help to identify the bonding strength between lignin and the ionic liquid and explain the property changes with lignin additives. In addition, the lignin/[CH][AA] ILs exhibit excellent non-corrosive features with both aluminum and iron boards. This work successfully demonstrates a new and important application of using lignin in bio-based ionic liquids as advanced non-corrosive green lubricants.

Acknowledgements

This work is financially supported by the start-up fund of The University of Akron. Partial support from Faculty Research Committee, Biomimicry Research Incentive Center, Firestone Faculty Research Fellowship of UAkron and National Natural Science Foundation of China (Grant No. 21306220) are also acknowledged.

References

1 D. Coleman and N. Gathergood, *Chem. Soc. Rev.*, 2010, **39**, 600–637.
2 M. V. Fedorov and A. A. Kornyshev, *Chem. Rev.*, 2014, **114**, 2978–3036.
3 T. Welton, *Chem. Rev.*, 1999, **99**, 2071–2084.
4 Q.-P. Liu, X.-D. Hou, N. Li and M.-H. Zong, *Green Chem.*, 2012, **14**, 304–307.
5 M. Petkovic, K. R. Seddon, L. P. N. Rebelo and C. S. Pereira, *Chem. Soc. Rev.*, 2011, **40**, 1383–1403.
6 A. George, A. Brandt, K. Tran, S. M. S. N. S. Zahari, D. Klein-Marcuschamer, N. Sun, N. Sathitsuksanoh, J. Shi, V. Stavila, R. Parthasarathi, S. Singh, B. M. Holmes, T. Welton, B. A. Simmons and J. P. Hallett, *Green Chem.*, 2015, **17**, 1728–1734.
7 F. Zhou, Y. Liang and W. Liu, *Chem. Soc. Rev.*, 2009, **38**, 2590–2599.
8 Y. Fukaya, Y. Iizuka, K. Sekikawa and H. Ohno, *Green Chem.*, 2007, **9**, 1155–1157.
9 J. K. Blusztajn, *Science*, 1998, **281**, 794–795.
10 J.-C. Plaquevent, J. Levillain, F. Guillen, C. Malhiac and A.-C. Gaumont, *Chem. Rev.*, 2008, **108**, 5035–5060.
11 K. Fukumoto, M. Yoshizawa and H. Ohno, *J. Am. Chem. Soc.*, 2005, **127**, 2398–2399.
12 K. D. Weaver, H. J. Kim, J. Sun, D. R. MacFarlane and G. D. Elliott, *Green Chem.*, 2010, **12**, 507–513.
13 X.-D. Hou, Q.-P. Liu, T. J. Smith, N. Li and M.-H. Zong, *PLoS One*, 2013, **8**, e59145.
14 X.-D. Hou, J. Xu, N. Li and M.-H. Zong, *Biotechnol. Bioeng.*, 2015, **112**, 65–73.

15 Z. Song, Y. Liang, M. Fan, F. Zhou and W. Liu, *RSC Adv.*, 2014, **4**, 19396–19402.
16 P. Moriel, E. J. Garcia-Suarez, M. Martinez, A. B. Garcia, M. A. Montes-Moran, V. Calvino-Casilda and M. A. Banares, *Tetrahedron Lett.*, 2010, **51**, 4877–4881.
17 X. Li, M. Hou, Z. Zhang, B. Han, G. Yang, X. Wang and L. Zou, *Green Chem.*, 2008, **10**, 879–884.
18 C. Ye, W. Liu, Y. Chen and L. Yu, *Chem. Commun.*, 2001, 2244–2245.
19 M. Palacio and B. Bhushan, *Tribol. Lett.*, 2010, **40**, 247–268.
20 S. Watanabe, K. Takiwatari, M. Nakano, K. Miyake, R. Tsuboi and S. Sasaki, *Tribol. Lett.*, 2013, **51**, 227–234.
21 H. Wang, Q. Lu, C. Ye, W. Liu and Z. Cui, *Wear*, 2004, **256**, 44–48.
22 T. Torimoto, T. Tsuda, K.-I. Okazaki and S. Kuwabata, *Adv. Mater.*, 2010, **22**, 1196–1221.
23 L. Zhang, J. Pu, L. Wang and Q. Xue, *ACS Appl. Mater. Interfaces*, 2015, **7**, 8592–8600.
24 A. Rahimi, A. Ulbrich, J. J. Coon and S. S. Stahl, *Nature*, 2014, **515**, 249–252.
25 A. J. Ragauskas, G. T. Beckham, M. J. Biddy, R. Chandra, F. Chen, M. F. Davis, B. H. Davison, R. A. Dixon, P. Gilna, M. Keller, P. Langan, A. K. Naskar, J. N. Saddler, T. J. Tschaplinski, G. A. Tuskan and C. E. Wyman, *Science*, 2014, **16**, 1246843.
26 W. Liu, R. Zhou, H. L. S. Goh, S. Huang and X. Lu, *ACS Appl. Mater. Interfaces*, 2014, **6**, 5810–5817.
27 J. Zhang, Y. Chen, P. Sewell and M. A. Brook, *Green Chem.*, 2015, **17**, 1811–1819.
28 Y. Sun, L. Yang, X. Lu and C. He, *J. Mater. Chem. A*, 2015, **3**, 3699–3709.
29 X. Pan, J. F. Kadla, K. Ehara, N. Gilkes and J. N. Saddler, *J. Agric. Food Chem.*, 2006, **54**, 5806–5813.
30 S. Zhou, L. Liu, B. Wang, F. Xu and R. Sun, *Process Biochem.*, 2012, **47**, 1799–1806.
31 M. J. Frisch, G. W. Trucks, H. B. Schlegel, G. E. Scuseria, M. A. Robb, J. R. Cheeseman, G. Scalmani, V. Barone, B. Mennucci, G. A. Petersson, H. Nakatsuji, M. Caricato, X. Li, H. P. Hratchian, A. F. Izmaylov, J. Bloino, G. Zheng, J. L. Sonnenberg, M. Hada, M. Ehara, K. Toyota, R. Fukuda, J. Hasegawa, M. Ishida, T. Nakajima, Y. Honda, O. Kitao, H. Nakai, T. Vreven, J. A. Montgomery, J. E. Peralta, F. Ogliaro, M. Bearpark, J. J. Heyd, E. Brothers, K. N. Kudin, V. N. Staroverov, R. Kobayashi, J. Normand, K. Raghavachari, A. Rendell, J. C. Burant, S. S. Iyengar, J. Tomasi, M. Cossi, N. Rega, J. M. Millam, M. Klene, J. E. Knox, J. B. Cross, V. Bakken, C. Adamo, J. Jaramillo, R. Gomperts, R. E. Stratmann, O. Yazyev, A. J. Austin, R. Cammi, C. Pomelli, J. W. Ochterski, R. L. Martin, K. Morokuma, V. G. Zakrzewski, G. A. Voth, P. Salvador, J. J. Dannenberg, S. Dapprich, A. D. Daniels, Ö. Farkas, J. B. Foresman, J. V. Ortiz, J. Cioslowski and D. J. Fox, *Gaussian 09, Revision C.01*, Gaussian, Inc., Wallingford, CT, 2009.
32 A. D. Becke, *Phys. Rev. A*, 1988, **38**, 3098–3100.
33 W. Yang and R. G. Parr, *Phys. Rev. B: Condens. Matter Mater. Phys.*, 1988, **37**, 785–789.
34 Y. Qian, X. Qiu and S. Zhu, *Green Chem.*, 2015, **17**, 320–324.
35 Y.-Y. Jiang, G.-N. Wang, Z. Zhou, Y.-T. Wu, J. Geng and Z.-B. Zhang, *Chem. Commun.*, 2008, 505–507.
36 H. H. A. Rahman, A. H. E. Moustafa and M. K. Awad, *Int. J. Electrochem. Sci.*, 2012, 1266–1287.

